Regenerative Therapy 16 (2021) 23–31

Contents lists available at ScienceDirect

Regenerative Therapy

journal homepage: http://www.elsevier.com/locate/reth

Original Article

CircRNA_25487 inhibits bone repair in trauma-induced osteonecrosis of femoral head by sponging miR-134-3p through p21

Ying Zhang [a, b, 1], Sansan Jia [a, c, 1], Qiushi Wei [d, e], Zhikun Zhuang [b], Jitian Li [a], Yanan Fan [a], Leilei Zhang [a], Zhinan Hong [d, e], Xianghao Ma [a], Ruibo Sun [a], Wei He [d, e], Haibin Wang [b], Youwen Liu [a, **], Wuyin Li [a, *]

[a] Medical Center of Hip, Luoyang Orthopedic-Traumatological Hospital (Orthopedics Hospital of Henan Province), Luoyang, 471002, Henan, China
[b] Guangzhou University of Traditional Chinese Medicine, Guangzhou, 510405, Guangdong, China
[c] Fujian University of Traditional Chinese Medicine, Fuzhou, 350122, Fujian, China
[d] Institute of Orthopaedics of Guangzhou University of Traditional Chinese Medicine, Guangzhou, 510240, China
[e] The Third Affiliated Hospital of Guangzhou University of Traditional Chinese Medicine, Guangzhou, 510240, China

ARTICLE INFO

Article history:
Received 4 November 2020
Received in revised form
25 November 2020
Accepted 9 December 2020

Keywords:
Trauma-induced osteonecrosis of femoral head
Circular RNA
microRNA
Proliferation

ABSTRACT

We aimed to identify specific circular RNAs (circRNAs) involved in bone repair of trauma-induced osteonecrosis of femoral head (TIONFH) and to explore the potential mechanism. CircRNA sequencing on the blood sample collected from patients with and without TIONFH was performed to select cirRNAs that were significantly differentially expressed, followed by qRT-PCR confirmation. Furthermore, the functions of one selected circRNA and the potential mechanisms in bone repair of TIONFH were validated based on the bone marrow mesenchymal stem cells (BMSCs) and osteoclast-like cells (OLCs) through CCK-8, flow cytometry, transwell assay, luciferase reporter assay, and western blot. A total of 234 upregulated and 148 downregulated differentially expressed circRNAs were identified, and qRT-PCR showed that circRNA_25487 was significantly upregulated in the peripheral blood of TIONFH patients. Luciferase reporter assay confirmed the binding effect between miR-134-3p and circRNA_25487. CircRNA_25487 suppression and miR-134-3p overexpression could promote cell proliferation and invasion while inhibited apoptosis of BMSCs and OLCs. miR-134-3p could target p21. CircRNA_25487 inhibited bone repair in TIONFH by sponging miR-134-3p to upregulate the expression of p21.

1. Introduction

Femoral neck fracture is an uncommon injury in the non-elderly people, which is often caused by high-energy trauma [1]. It is estimated that the number of hip fractures worldwide would increase from 1.66 million in 1990 to 6.26 million by 2050, representing an growing burden on healthcare [2]. Trauma-induced osteonecrosis of femoral head (TIONFH), the most common aseptic osteonecrosis of femoral head (ONFH) caused by hip dislocation, femoral neck fractures, and other hip trauma, is a main complication of femoral neck fractures [3]. It has been reported that fracture reduction and internal fixation can promote fracture healing, but it cannot completely prevent the occurrence of TIONFH. Many failures of internal fixation are associated with necrosis [4]. Currently, the molecular mechanism related to bone repair in patients with TIONFH is still unclear.

* Corresponding author. Medical Center of Hip, Luoyang Orthopedic-Traumatological Hospital (Orthopedics Hospital of Henan Province), No. 82 Qiming South Road, Luoyang, 471002, Henan, China.
** Corresponding author. Medical Center of Hip, Luoyang Orthopedic-Traumatological Hospital (Orthopedics Hospital of Henan Province), No. 82 Qiming South Road, Luoyang, 471002, Henan, China.
E-mail addresses: 61095864@qq.com (Y. Zhang), 2034768442@qq.com (S. Jia), Weiqshi@126.com (Q. Wei), 851642964@qq.com (Z. Zhuang), Jitianlee@hotmail.com (J. Li), 741363504@qq.com (Y. Fan), 527959217@qq.com (L. Zhang), hzn020@qq.com (Z. Hong), 992372739@qq.com (X. Ma), 542344857@qq.com (R. Sun), hw13802516062@163.com (W. He), 18408758@qq.com (H. Wang), liuyouwen2000@163.com (Y. Liu), liwuyin2000@163.com (W. Li).
Peer review under responsibility of the Japanese Society for Regenerative Medicine.
[1] Contributed equally to this work.

https://doi.org/10.1016/j.reth.2020.12.003

Circular RNAs (circRNAs) are new members of non-coding RNAs that are derived from exons with closed continuous loop structure. Compared with their linear counterparts, the circRNAs are highly stable [5–7]. Recently, studies have demonstrated that circRNAs are closely associated with the cell proliferation and apoptosis by sponging miRNAs to regulate gene expression [5,8,9]. A recent study of Kuang et al. [10] proved that circUSP45 could decrease osteogenesis in glucocorticoid-induced ONFH by sponging miR-127-5p. However, to our best knowledge, no study has reported the functions of circRNAs in TIONFH.

Therefore, in this study, we aimed to identify specific circRNAs involved in bone repair of TIONFH and to explore the potential mechanism. With this purpose, we performed circRNA sequencing on the blood sample collected from patients with and without TIONFH to select cirRNAs that were significantly differentially expressed. Furthermore, we validated the functions of one selected circRNA in bone repair of TIONFH based on the bone marrow mesenchymal stem cells (BMSCs) and osteoclast-like cells (OLCs). Our study may provide a foundation for diagnosis and treatment of TIONFH.

2. Materials and methods

2.1. Clinical sample data

Since January 2015 to April 2015, six patients (without gender limitations) with femoral neck fractures who developed ONFH after treatment with manual reduction and percutaneous cannulated screw fixation in the Henan Orthopaedic Hospital Hip Disease Treatment Study Centre were involved in this study. These patients were in line with the diagnostic criteria of ONFH [11]. Additionally, six age-matched patients with simple femoral neck fractures who received percutaneous internal fixation and did not developed ONFH were included as control. There was no statistical difference in age between the two groups.

None of the patients received drug treatment in the past six months, and they did not have other joint diseases, autoimmune disease, systemic inflammation, malignant or chronic diseases, such as rheumatoid arthritis, gout, a history of knee trauma, joint infection systemic lupus erythematosus, psoriasis, or hemophilia.

All patients underwent bilateral hips joint X-ray of frog-leg and orthotopic position, and bilateral hip magnetic resonance imaging (MRI) examination. Elbow venous blood samples were collected from all subjects during fasting and stored at −80 °C.

This study was fully in accordance with the relevant provisions of the 1964 Helsinki Declaration. This study was approved by the clinical trials ethics committee of Luoyang Orthopaedic-Traumatological Hospital of Henan Province (Henan Provincial Orthopedic Hospital) (institutional approval number: 81473704). All patients had provided the written consent from each clinical subject.

2.2. Total RNA extraction and library construction

Total RNA of was isolated from each blood sample using TRIzol reagent (Invitrogen, USA). RNA degradation and contamination were monitored by agarose gels (1%). Total RNA purity was checked using Nanodrop. RNA integrity was evaluated by Agilent 2100 Bioanalyzer (Agilent Technologies, USA).

The ribosomal RNA (rRNA) was removed from total RNA using Illumina epicentre ribo-zero kit (Illumina, USA). Purified RNA (polyA + and polyA-) was fragmented using fragmentation Buffer) and then the fragmented circRNA was used as template to synthesize cDNA based on the random hexamers. Double-stranded cDNA synthesis was then performed with dNTPs, RNaseH and DNA Polymerase I. The DNA fragments were end-repaired using T4 DNA polymerase and Klenow DNA polymerase, followed by polyadenylation at the 3' end and purification using AMPure XP beads (Beckman Coulter, USA). After that, USER enzyme was used to degrade the second strand of cDNA containing U. Finally, PCR amplification was performed to obtain the final sequencing library. Illumina Hiseq4000 was used for sequencing, which produced the paired-end libraries with 150 bp (PE150) read length.

2.3. Differentially expressed circRNAs identification

After quality control and reference genome alignment, differentially expressed circRNAs between TIONFH group and patients without TIONFH after femoral neck fracture were identified with $|\log2 \text{ fold change}| > 1$ and p value < 0.05. Then cluster analysis was carried out for differentially expressed circRNAs to intuitively show the expression of genes in different samples.

2.4. qRT-PCR

Total RNA was extracted from samples using RNA Isolater Total RNA Extraction Reagent (Vazyme, Nanjing, China). cDNA was synthesized by the GoScript Reverse transcription (RT) System (Promega, WI, USA). The expression levels of circRNA_25775, circRNA_33798, circRNA_25487, circRNA_18052 and circRNA_3684 were analyzed using the CFX96 Q-PCR Detection System (Bio-Rad, CA, USA). The reaction system with 14 μL volume consisted of 3 μL of cDNA, 1.4 μL of primers, 7 μL of AceQ qPCR SYBR Green Master Mix (Vazyme Biotech Co., NJ, USA), and 0.4 μL of ultrapure water. The relative expression levels were calculated by relative quantification ($2^{-\Delta\Delta Ct}$) method.

2.5. BMSCs culture

The Sprague-Dawle (SD) rats (purchased from Institute of Model Organism in Nanjing University, China) were killed by neck fracture, and soaked in 75% ethyl alcohol for 5 min, and then transferred to bechtop. The long bones (femur and tibia) of the mice were isolated under aseptic conditions and soaked in PBS solution. The femur and tibia were deeply dissected to remove the attached muscle tissue, and the metaphysis. The bone marrow cavity was repeatedly rinsed with 10% fetal bovine serum (FBS) and IMDM medium (Gibco; 12440053) until the bone marrow cavity turned white. The washing liquid was collected, and gently blown into individual cells by the pipette. The cells were inoculated in a six-well plate and cultured in a 37 °C incubator with 5% CO_2. The six-well plate was not moved during the culture to make BMSCs fully adherent to the wall. After 48 h of culture, the cells were gently washed with preheated PBS buffer for 2 times, and fresh medium was added. After that, the medium was changed every 48 ho. After 6–7 d of primary culture, cells were subcultured.

2.6. OLCs culture

The 4-week-old Wistar rats were rinsed with distilled water and killed by neck fracture. After soaking in 75% ethyl alcohol for 5 min, femur, tibia, humerus and radius were isolated with ophthalmic instruments. Following carefully removing the soft tissue around the bone, epiphysis was cut off, and the diaphysis was washed twice with α-MEM culture solution (Hylcone; SH30265.01B), and then placed in cold α-MEM culture solution. Then the marrow cavity was washed with α-MEM, and cells mixture was collected and inoculated into the cell culture plate (3.5 mm in diameter), and then cultured in 5% CO_2 incubator (37 °C) for 30 min. After 30 min, the culture solution (containing myelomoncyte) was centrifuged at 800

r/min for 8 min at 4 °C. The precipitation was resuspended with medium containing 10^{-8} mol/L of $25(OH)_2D_3$ α-MEM. The cell density was adjusted to 2.5×10^5/ml, and inoculated to 24-well plates (osteoblasts had been inoculated beforehand). The plates were cultured in 5% CO_2 incubator (37 °C), and 50% medium was changed every 48h. After 6–7 d of primary culture, cells were subcultured.

2.7. Target gene prediction

Targetscan (http://www.targetscan.org/) [12] and miRanda (http://www.microrna.org/microrna/home.do) [13] were used to predict the potential miRNA binding sites of circRNA_25487. The target gene of miR-134-3p was predicted by miRanda.

2.8. Cell transfection

Cells were seeded on six-well plates at a density of 3×10^5 in order to reach 30–50% confluence and miR-134-3p mimic (ugugacugguugaccagagggg) and si-circRNA_25487 (ACAGACAAGATTGAGGTACAT) were subcloned into the modified pcDNA3 (+) vector (Invitrogen, USA). Cells were also transfected with the corresponding negative control vectors using Lipofectamine 3000 (Thermo Fisher Scientific, USA). The miRNA mimic and negative control were obtained from RiboBio Biotechnology (Guangzhou, China). Then cells were harvested after 48 h for the validation of miR-134-3p overexpression by using qRT-PCR analysis.

2.9. Luciferase reporter assays

To construct a luciferase reporter for wild-type (WT) miR-134-3p, miR-329-5p, miRNA-411-5p, miR-149-3p, miR-485-5p and miR-30b-3p 3′UTR, the UTR sequences were synthesized and subcloned into the NotI and XhoI sites in the apsiCHECK-2 vector (Promega). To design apsiCHECK-2 plasmid, the DNA sequences were synthesized and subcloned in to apsiCHECK-2. Then bacteria were lysed and plasmids were harvested. The mutant 3′UTR was produced by site-directed mutagenesis using Phusion™ High-Fidelity DNA Polymerase (Thermo Fisher Scientific). For transfection, 5×10^4 293T cells were plated on a 24-well plate with complete medium. After 24 h, cells were transfected with 50 nM of pcDNA3.0-ciR25487 or NC pcDNA3.0 using Lipofectamine 3000 (Thermo Fisher Scientific) and were harvested after 72 h of transfection for luciferase activity detection using the Dual-Luciferase Reporter Assay System (Beyotime, Shanghai). Similar methods were used to determine the regulatory relation between miR-134-3p and p21.

2.10. Cell proliferation assay

Cell proliferation was measured with a Cell Counting Kit-8 (CCK-8; Dojindo, Japan). Briefly, the cells were seeded in 96-well culture plates at a density of 5×10^3/well. Cell viability was then determined using the CCK8 at 24, 48, and 72 h after transfection. The absorbance at 570 nm was measured with a microplate reader (BioTek, USA).

2.11. Apoptosis assay

BMSCs and OLCs were seeded at a density of 3×10^5 cells/well in 6-well plates. After 48 h of transfection, BMSCs and OLCs were collected by trypsinization. Then BD Pharminge™ FITC-Annexin V Apoptosis Detection Kit (BD Biosciences, USA) was applied to perform Annexin V/PI staining according to the manufacture's instruction. The apoptotic rates of each sample were analyzed using a flow cytometer (ACSCalibur, Becton Dickinson, San Jose, CA).

2.12. Transwell assay

As to the transwell analysis, OLC and BMSC cells (1.0×10^5) in 100 μL of serum-free medium were incubated for the (non-) Matrigel-coated upper chamber (8-μm pore size, BD Falcon cell culture inserts, BD Biosciences, USA) following the manufacturer's instruction. Total 500 μL of 10% FBS containing medium was added to the lower chamber. After 24 h incubation, non-migrated/invaded cells on the upper surface were removed with a cotton swab and cells migrated to the lower chamber were fixed with 4% methanol, and stained with crystal violet staining solution. The number of migrated cells was counted under a microscope (DM IL, Leica Microsystems) in five random fields and calculated as the average per field.

2.13. Western blotting

The cells were washed and total proteins were extracted using RIPA buffer (Beyotime, Shanghai, China). Cell membrane protein was obtained using a Cell Membrane Protein Extraction Kit (XY-Bioscience, Shanghai, China). Cytoplasmic protein was obtained using a Nuclear and Cytoplasmic Protein Extraction Kit (Kamimi Yasuro Biological Technology, Shanghai, China). The protein concentrations were normalized using a BCA protein assay (Thermo Fisher Scientific). Total 30 μg lysate proteins were separated using 10% SDS-PAGE gels, and then transferred to PVDF membranes (Millipore, Darmstadt, Germany). The membranes were blocked with 5% nonfat milk in TBST for 1 h and incubated with specific primary antibodies (p21 (Santa Cruze; sc-6246), GAPDH (abcam; ab9485)) overnight at 4 °C. Then the membranes were incubated with horseradish peroxidase-

Table 1
Basic information for TIONFH patients and patients without necrosis.

Factors	Non-necrosis group (n = 6)	Necrosis group (n = 6)	$t/\chi^2/Z$	P value
Age (years)	48.00 ± 7.75	47.00 ± 9.42	0.201	0.845
Sex (male/female)	3/3	5/1	1.552	0.213
BMI (g)	24.61 ± 3.34	25.25 ± 3.18	−0.337	0.743
Body temperature (℃)	36.77 ± 0.41	36.57 ± 0.37	0.892	0.393
Pulse (time/min)	76.50 ± 1.52	77.00 ± 4.86	−0.241	0.818
Breathe (time/min)	18.50 ± 1.05	19.00 ± 0.90	−0.889	0.395
Systolic blood pressure (mmHg)	123.83 ± 10.46	119.33 ± 6.56	0.893	0.393
Diastolic blood pressure (mmHg)	81.33 ± 6.19	81.17 ± 4.22	0.055	0.958

t, Statistical value of independent-samples T test; χ2, Statistical value of Chi-squared; Z, Statistical value of Mann-Whitney Test.

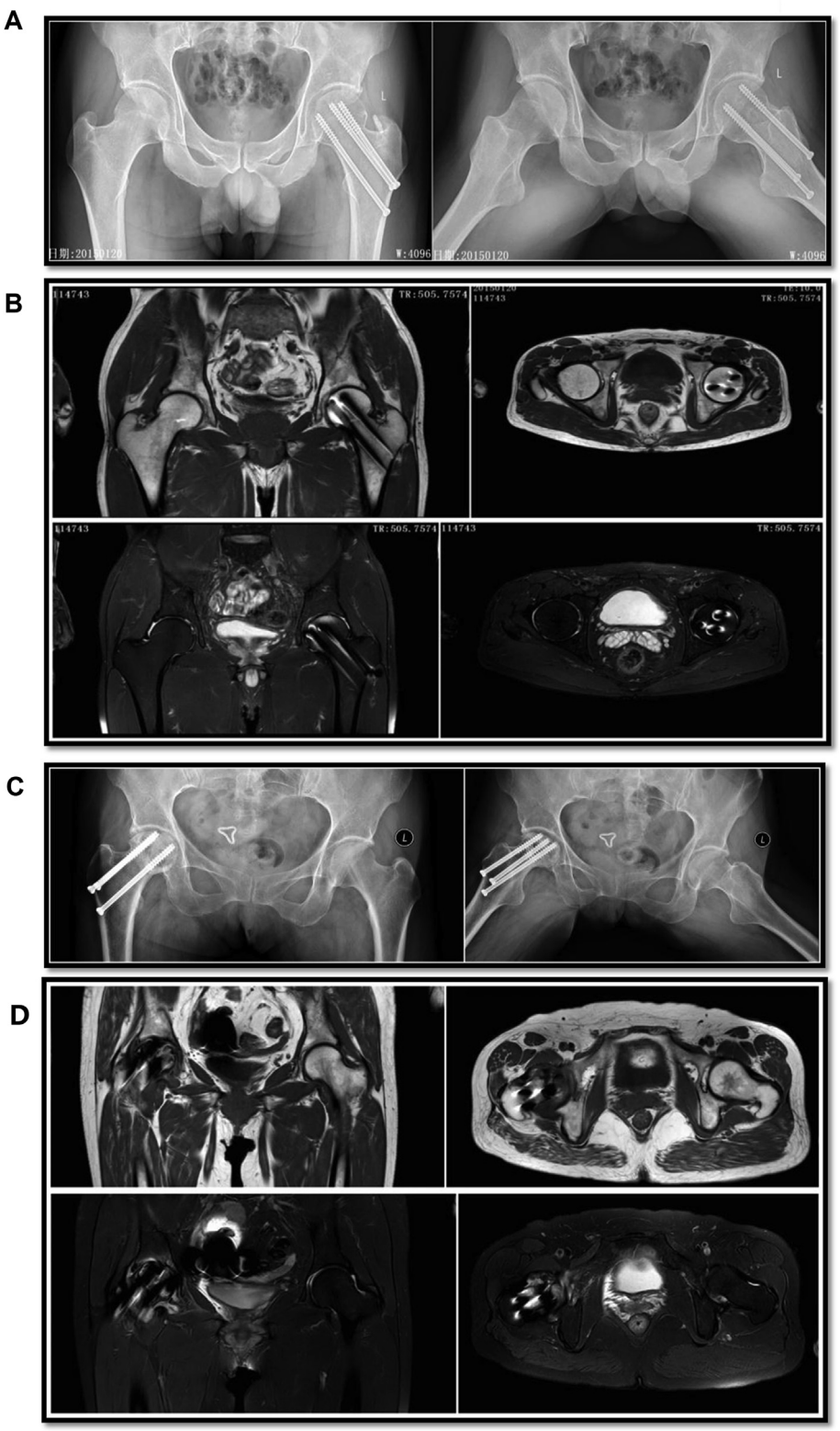

Fig. 1. MRI and X-ray examination of TIONFH patients and the patients without TIONFH. (A) X-ray of patients without necrosis showed a smooth surface without collapse. (B) MRI of patients without necrosis showed hollow spike-like images without a significant "double line". (C) X-ray of necrosis patients showed femoral head collapse, density changes, cystic changes, or hollow or pierced femoral head surface. (D) MRI of necrosis patients showed a clear "double line" sign and displayed high signals on fat-suppressed images.

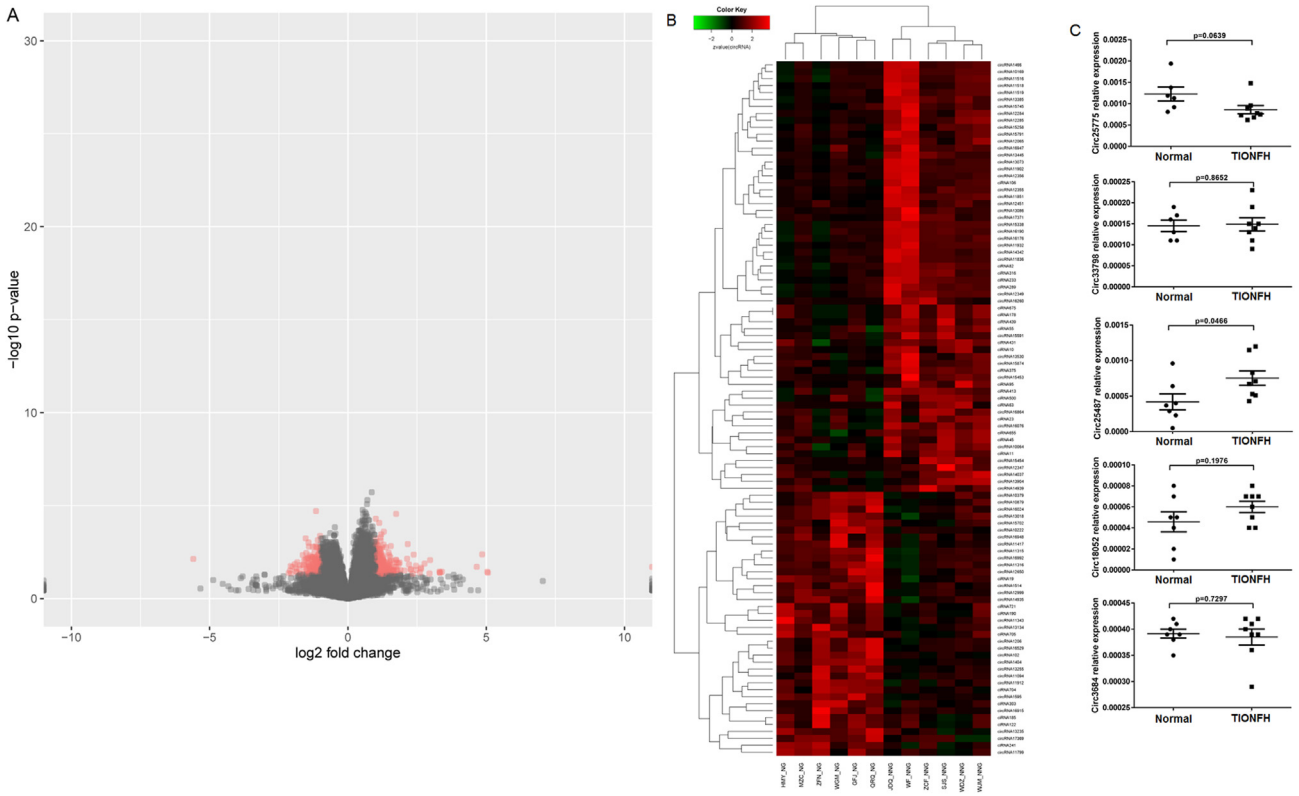

Fig. 2. (A) Heatmap of differentially expressed circRNAs. (B) Relative expression levels of circRNA_25775, circRNA_33798, circRNA_25487, circRNA_18052 and circRNA_3684 in blood samples of two groups detected by qRT-PCR.

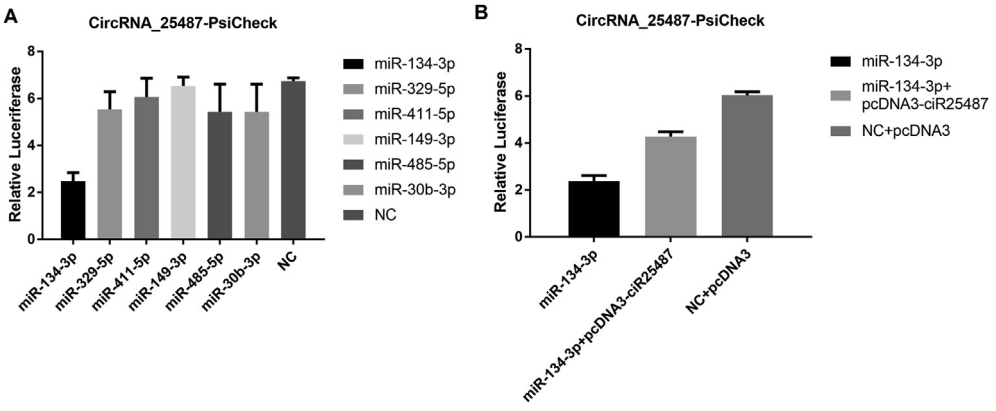

Fig. 3. (A) The relative luciferase activities of six miRNAs, and (B) miR-134-3p had interaction with circRNA 25487-psicheck.

labeled secondary antibodies for 1 h at room temperature. A SuperSignal® WestDura Extended Duration Substrate was applied to visualize the protein bands.

2.14. Statistical analysis

All data are shown as mean ± standard deviation. Statistical analyses were conducted using SPSS 19.0 statistical software (SPSS Inc., Chicago, IL). Data between two groups were analyzed using t tests, and multiple comparisons between groups were analyzed by one-way ANOVA. $P < 0.05$ was considered statistically significant.

3. Results

3.1. Clinical data and X-ray and MRI examinations

Clinical data of 12 patients are shown in Table 1. There were no significant differences for the two groups of patients in age, sex, MBI, blood pressure and other vital signs. In patients without ONFH, the surface of femoral head was smooth without collapse (Fig. 1A). There appeared hollow spike-like images without a significant “double line” sign (Fig. 1B). Patients with ONFH showed femoral head collapse or density changes, cystic changes, or a hollow or pierced femoral head surface (Fig. 1C).

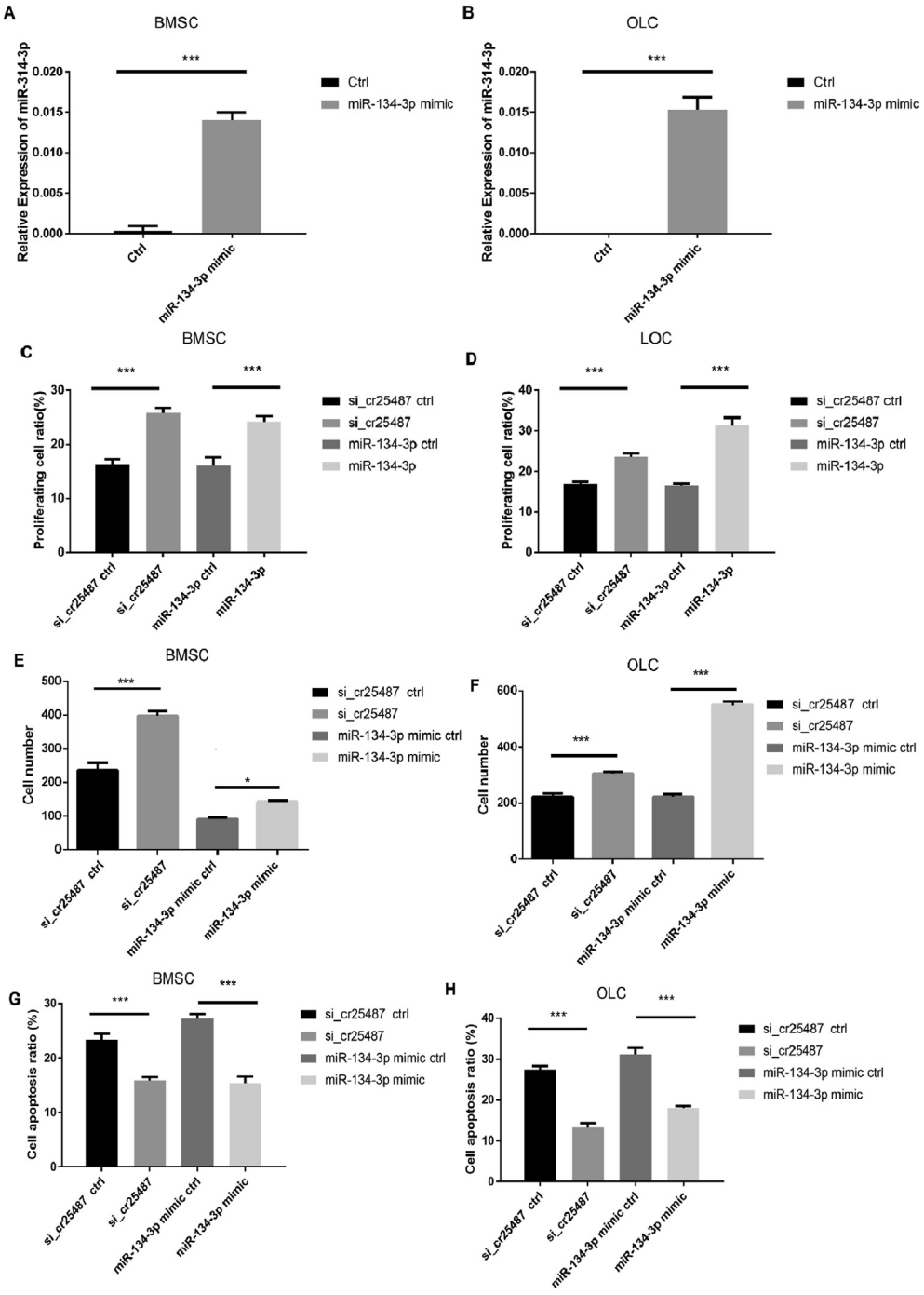

Fig. 4. (A and B) Relative expression levels of miR-134-3p in BMSCs and OLCs after cells were transfected with miR-134-3p mimic. (C and D) Proliferation rates of BMSCs and OLCs after circRNA_25487 suppression and miR-134-3p overexpression. (E and F) Invasion of BMSCs and OLCs after circRNA_25487 suppression and miR-134-3p overexpression. (G and H) Apoptosis rates of BMSCs and OLCs after circRNA_25487 suppression and miR-134-3p overexpression. *P < 0.05, ***P < 0.001 compared with control.

Additionally, there was a clear “double line” sign and high signals on fat-suppressed images (Fig. 1D) [3].

3.2. Differentially expressed circRNAs identification and qRT-PCR confirmation

A total of 234 upregulated and 148 downregulated differentially expressed circRNAs were identified. The volcano plot and heatmap of differentially expressed circRNAs are shown in Fig. 2A and B. Among these differentially expressed circRNAs, circRNA_25775, circRNA_33798, circRNA_25487, circRNA_18052 and circRNA_3684 had significant differences between two groups (|log2 fold change| > 1 and p value < 0.05). qRT-PCR was carried out to validate the expression levels of the five cirRNAs in blood samples of two groups and the results showed that circRNA_25487 was significantly upregulated in the peripheral blood of TIONFH patients (Fig. 2C), which was consistent with the sequencing results.

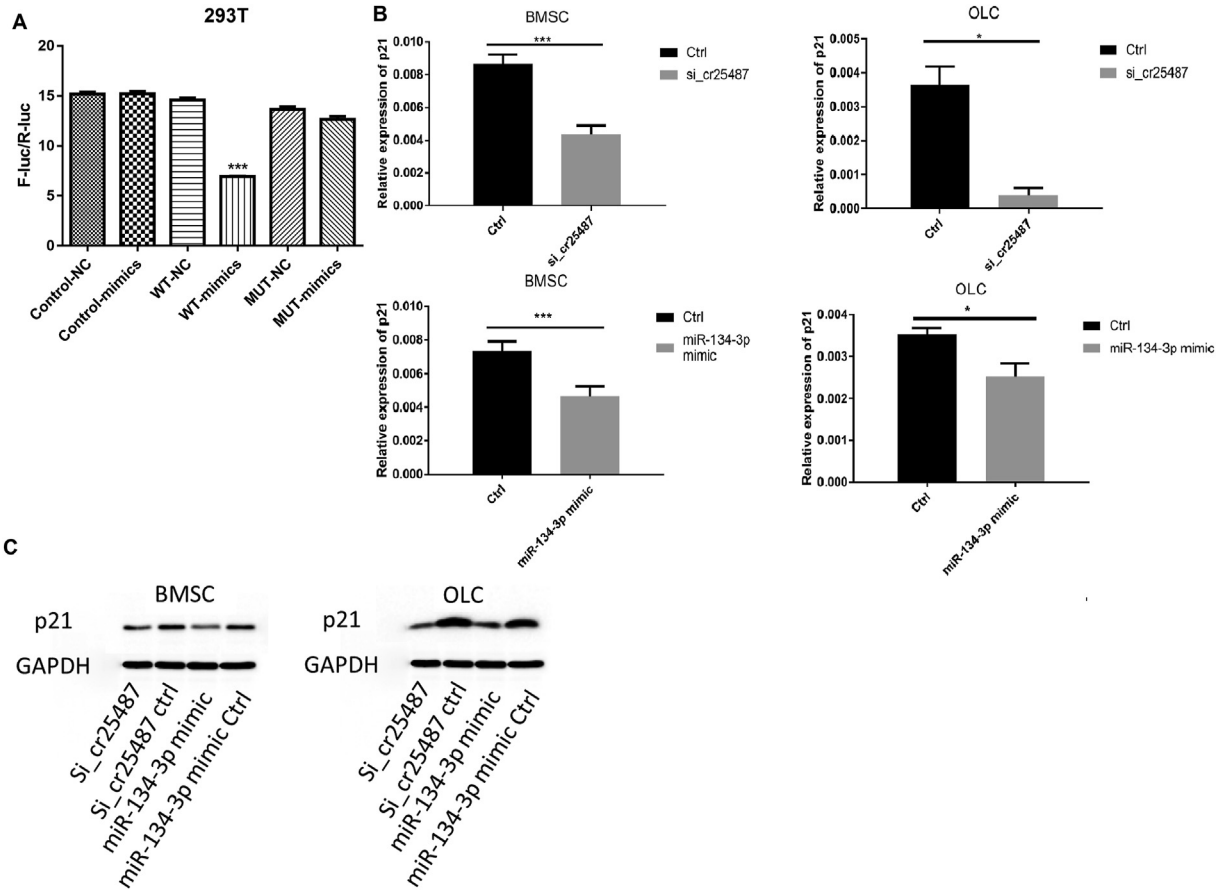

Fig. 5. (A) The regulatory relation between miR-134-3p and p21. Co-transfection of miR-134-3p mimics and wild-type reporter gene plasmid significantly decreased the luciferase activity. (B and C) The mRNA and protein expression of p21 after circRNA_25487 suppression and miR-134-3p overexpression. *P < 0.05, ***P < 0.001 compared with control.

3.3. miRNA binding site prediction and validation for circRNA_25487

miR-134-3p, miR-329-5p, miRNA-411-5p, miR-149-3p, miR-485-5p and miR-30b-3p were predicted for circRNA_25487. Luciferase reporter assay showed that the relative luciferase activity of miR-134-3-p decreased significantly compared with the other miRNAs, suggesting that miR-134-3-p had interaction with circRNA 25487-psicheck (Fig. 3A). The binding effect between miR-134-3p and circRNA_25487 was further confirmed (Fig. 3B).

3.4. Effect of circRNA_25487 suppression and miR-134-3p overexpression on cell proliferation, invasion and apoptosis

The transfection effect of miR-134-3p mimics is shown in Fig. 4A and B. The relative expression level of miR-134-3p increased significantly in both BMSCs and OLCs after cell transfection ($P < 0.001$). The proliferation rates of BMSCs and OLCs after circRNA_25487 suppression and miR-134-3p overexpression are shown in Fig. 4C and D. The results showed that both circRNA_25487 suppression and miR-134-3p overexpression significantly increased the proliferation rates of BMSCs and OLCs ($P < 0.001$). Additionally, transwell assay revealed that suppression of circRNA_25487 and overexpression of miR-134-3p could significantly promote the invasion of BMSCs and OLCs ($P < 0.001$ or $P < 0.05$) (Fig. 4E and F). The apoptosis rates of the two types of cells significantly decreased in circRNA_25487 suppression and miR-134-3p overexpression groups ($P < 0.001$) (Fig. 4G and H).

3.5. miRNA-134-3p target gene prediction

miRanda was used to predict the potential targets of miRNA-134-3p, and we finally focused on p21 due to its role in cell proliferation. The regulatory relation between miRNA-134-3p and p21 was further confirmed by luciferase reporter assay. As shown in Fig. 5A, The wild-type 3′-UTR sequence and the mutant 3′-UTR sequence of p21 were cloned to construct reporter plasmids and mutant vectors, respectively. We found that co-transfection of miR-134-3p mimics and wild-type reporter gene plasmid significantly decreased the luciferase activity. On the contrary, there was no significant difference in luciferase activity between miR-134-3p co-transfected mimics and mutant plasmids. Moreover, the expression level of p21 after circRNA_25487 suppression or miR-134-3p overexpression was detected through qRT-PCR and western blot. As shown in Fig. 5B, the relative expression of p21 mRNA significantly decreased after circRNA_25487 suppression or miR-134-3p overexpression in both BMSCs ($P < 0.001$) and OLCs ($P < 0.05$). Western blot analysis showed similar results (Fig. 5C).

4. Discussion

TIONFH is a blood circulation disorder of the femoral head, with a variety of etiologies that can lead to the death of bone cells and bone marrow components, thereby causing structural changes of the femoral head [3]. Therefore, investigation of BMSCs proliferation is critical for the treatment of this disease. In this study, the potential mechanism of TIONFH patient bone collapse was

explored through circRNA sequencing, and circRNA_25487 was demonstrated to be upregulated in patients with TIONFH compared with without TIONFH. Further studies revealed that circRNA_25487 inhibited the proliferation of BMSCs and OLCs by sponging miR-134-3p to regulate p21 expression.

Recent studies on ONFH have focused on the epigenetic regulation of its pathogenesis, specifically on non-coding RNAs, such as long noncoding RNAs, miRNAs, and circRNAs [14–16]. However, the exact mechanism of circRNAs in the pathogenesis of TIONFH is largely unknown. Recently, due to the multiple biological functions of circRNAs in bone remodeling, they have attracted more and more attention. Our study, for the first time, reported the function of circRNA_25487 in regulating the proliferation of BMSCs and OLCs for the treatment of TIONFH.

In the non-coding RNA cluster, circRNAs are relative new biomarkers, which is found to play important roles in metabolic activities like cell cycle regulation, and immune surveillance [17]. For instance, circTCF25 could sponge miR-107 to upregulate 13 targets related with cell proliferation, migration and invasion [18]. circRNA_LARP4 can inhibit cell proliferation and invasion by sponging miR-424-5p to regulate LATS1 expression in gastric cancer [5]. A more recent study showed that as a miR-7 inhibitor, circRNACDR1 can trigger the upregulation of GDF5 and subsequent phosphorylation of p38 MAPK and Smad1/5/8, thereby promoting the osteogenic differentiation of periodontal ligament stem cells [19]. In the present study, we found that circRNA_25487 level was increased in TIONFH patients compared with control. Additionally, circRNA_25487 suppression promoted the proliferation and inhibited the apoptosis of BMSCs and OLCs. The mesenchymal stem cells (MSCs) have emerged as promising candidates for orthopedic applications. BMSCs are considered as the progenitors for skeletal tissues, and these cells have been demonstrated to have a great potential for bone repair [20]. Additionally, osteoclasts have been reported to modulate osteogenesis [21]. Thus, we speculated that circRNA_25487 may act as a biomarker to regulate the bone repair in TIONFH.

Furthermore, we investigated the potential mechanisms of circRNA_25487 in TIONFH, and found that circRNA_25487 directly interacted with miR-134-3p. Following that, we investigated the sponge function of circRNA_25487 and revealed that circRNA_25487/miR-134-3p/p21 may be a cascade to regulate bone repair in TIONFH. miR-134 has been reported to function as a regulator of cell proliferation and apoptosis. Overexpression of miR-134 could suppress cell proliferation in some human cancers [22,23], while overexpressed miR-134 promotes cell proliferation in neurons [24], which suggested a diverse functions of this miRNA. p21, a p53-inducible protein, is responsible for a bifurcation in cyclin dependent kinase 2 activity following mitosis, and that this underpins the proliferation-quiescence decision in cycling cells [25,26]. P21 is downregulated in various cancers [27], and plays important roles in multiple cellular processes during unperturbed cell growth by binding directly to G1/S transition-related kinases [28,29]. Importantly, Yew et al. [30] have reported that knockdown of p21 in late-passage MSCs exhibits increased proliferation capacity and increased osteogenic potential. Using $p21^{(-/-)}$ knockout mice, a recent study of Premnath et al. [31] also provided a strong rationale to examine the role of p21 in bone repair. In our study, inhibited circRNA_25487 and overexpressed miR-134-3p downregulated the expression level of p21, which was verified by qRT-PCR and western blot. Given the important role of p21 in cell proliferation, we further confirmed the critical roles of circRNA_25487 in TIONFH by regulating the proliferation of BMSCs and OLCs.

5. Conclusions

In conclusion, circRNA_25487 inhibited bone repair in TIONFH by sponging miR-134-3p to upregulate the expression of p21. The findings provide a new target for diagnosis and treatment of TIONFH.

Ethical approval

This study was approved by the clinical trials ethics committee of Luoyang Orthopaedic-Traumatological Hospital of Henan Province (Henan Provincial Orthopedic Hospital).

Informed consent

The written consent form was obtained from each clinical subject.

Availability of data and materials

All data generated or analysed during this study are included in this published article.

Declaration of competing interest

The authors declare that they have no known competing financial interests or personal relationships that could have appeared to influence the work reported in this paper.

Authors' contributions

Conception and design of the research: YZ, SJ, WL; acquisition of data: ZZ, YF, ZH, YL; analysis and interpretation of data: LZ, XM, RS; statistical analysis: QW, JL; obtaining funding: YZ, WL; drafting the manuscript: YZ, SJ; revision of manuscript for important intellectual content: WH, HW. All authors read and approved the final manuscript.

Acknowledgements

This work was supported by National Science Foundation of China (grant number 81774348 and 81874477).

References

[1] M P, R P, G Pv. Biomechanical rationale for implant choices in femoral neck fracture fixation in the non-elderly. Injury 2015;46(3):445–52.
[2] Dennison E, Mohamed MA, Cooper C. Epidemiology of osteoporosis. Rheum Dis Clin 2006;32(4):617–29.
[3] Zhang Y, Wei QS, Ding WB, Zhang LL, Wang HC, et al. Increased microRNA-93-5p inhibits osteogenic differentiation by targeting bone morphogenetic protein-2. PloS One 2017;12(8):e0182678.
[4] Bonfiglio M, Yoke EM. Aseptic necrosis of the femoral head and non-union of the femoral neck: effect of treatment by drilling and bone-grafting (Phemister technique). JBJS 1968;50(1):48–66.
[5] Zhang J, Liu H, Hou L, Wang G, Zhang R, Huang Y, et al. Circular RNA_LARP4 inhibits cell proliferation and invasion of gastric cancer by sponging miR-424-5p and regulating LATS1 expression. Mol Canc 2017;16(1):151.
[6] Greene J, Baird A, Brady L, Lim M, Gray SG, McDermott R, et al. Circular RNAs: biogenesis, function and role in human diseases. Front Molec Biosci. 2017;4:38.
[7] Kulcheski FR, Christoff AP, Margis R. Circular RNAs are miRNA sponges and can be used as a new class of biomarker. J Biotechnol 2016;238:42–51.
[8] Wang R, Zhang S, Chen X, Li N, Li J, Jia R, et al. CircNT5E acts as a sponge of miR-422a to promote glioblastoma tumorigenesis. Canc Res 2018;78(17):4812–25.
[9] Xie H, Ren X, Xin S, Lan X, Lu G, Lin Y, et al. Emerging roles of circRNA_001569 targeting miR-145 in the proliferation and invasion of colorectal cancer. Oncotarget 2016;7(18):26680.
[10] Kuang M-j, Xing F, Wang D, Sun L, Ma JX, Ma XL. CircUSP45 inhibited osteogenesis in glucocorticoid-induced osteonecrosis of femoral head by

sponging miR-127-5p through PTEN/AKT signal pathway: experimental studies. Biochem Biophys Res Commun 2019;509(1):255–61.
[11] Zhao Dw, Hu Yc. Chinese experts' consensus on the diagnosis and treatment of osteonecrosis of the femoral head in adults. Orthop Surg 2012;4(3):125–30.
[12] Lewis BP, Burge CB, Bartel DP. Conserved seed pairing, often flanked by adenosines, indicates that thousands of human genes are microRNA targets. Cell 2005;120(1):15–20.
[13] Bentwich I. Prediction and validation of microRNAs and their targets. FEBS Lett 2005;579(26):5904–10.
[14] Xu D, Gao Y, Hu N, Wu L, Chen Q. miR-365 ameliorates dexamethasone-induced suppression of osteogenesis in MC3T3-E1 cells by targeting HDAC4. Int J Mol Sci 2017;18(5):977.
[15] Shi C, Qi J, Huang P, Jiang M, Zhou Q, Zhou H, et al. MicroRNA-17/20a inhibits glucocorticoid-induced osteoclast differentiation and function through targeting RANKL expression in osteoblast cells. Bone 2014;68:67–75.
[16] Liang D, Wilusz JE. Short intronic repeat sequences facilitate circular RNA production. Genes Dev 2014;28(20):2233–47.
[17] Matsumoto A, Pasut A, Matsumoto M, Yamashita R, Fung J, Monteleone E, et al. mTORC1 and muscle regeneration are regulated by the LINC00961-encoded SPAR polypeptide. Nature 2017;541(7636):228.
[18] Zhong Z, Lv M, Chen J. Screening differential circular RNA expression profiles reveals the regulatory role of circTCF25-miR-103a-3p/miR-107-CDK6 pathway in bladder carcinoma. Sci Rep 2016;6:30919.
[19] Li X, Zheng Y, Zheng Y, Huang Y, Zhang Y, Jia L, et al. Circular RNA CDR1as regulates osteoblastic differentiation of periodontal ligament stem cells via the miR-7/GDF5/SMAD and p38 MAPK signaling pathway. Stem Cell Res Ther 2018;9(1):232.
[20] Wang A, Ren M, Song Y, Wang X, Wang Q, Yang Q, et al. MicroRNA expression profiling of bone marrow mesenchymal stem cells in steroid-induced osteonecrosis of the femoral head associated with osteogenesis. Med Sci Mon Int Med J Exp Clin Res: Int Med J Exp Clin Res 2018;24:1813.
[21] Lossdörfer S, Schwartz Z, Wang L, Lohmann CH, Turner JD, Wieland M, et al. Microrough implant surface topographies increase osteogenesis by reducing osteoclast formation and activity. J Biomed Mater Res Part A: Offic J Soc Biomat Japan Soc Biomat Austr Soc Biomat Korean Soc Biomat 2004;70(3):361–9.
[22] Liu Y, Zhang M, Qian J, Bao M, Meng X, Zhang S, et al. miR-134 functions as a tumor suppressor in cell proliferation and epithelial-to-mesenchymal Transition by targeting KRAS in renal cell carcinoma cells. DNA Cell Biol 2015;34(6):429–36.
[23] Li J, Wang Y, Luo J, Fu Z, Ying J, Yu Y, et al. miR-134 inhibits epithelial to mesenchymal transition by targeting FOXM1 in non-small cell lung cancer cells. FEBS Lett 2012;586(20):3761–5.
[24] Gaughwin P, Ciesla M, Yang H, Lim B, Brundin P, et al. Stage-specific modulation of cortical neuronal development by Mmu-miR-134. Cerebr Cortex 2011;21(8):1857–69.
[25] Spencer SL, Cappell SD, Tsai FC, Overton KW, Wang CL, Meyer T, et al. The proliferation-quiescence decision is controlled by a bifurcation in CDK2 activity at mitotic exit. Cell 2013;155(2):369–83.
[26] Xiong Y, Hannon GJ, Zhang H, Casso D, Kobayashi R, Beach D. p21 is a universal inhibitor of cyclin kinases. Nature 1993;366(6456):701.
[27] Abbas T, Dutta A. p21 in cancer: intricate networks and multiple activities. Nat Rev Canc 2009;9(6):400.
[28] Gartel AL, Radhakrishnan SK. Lost in transcription: p21 repression, mechanisms, and consequences. Canc Res 2005;65(10):3980–5.
[29] Sherr CJ, Roberts JM. Inhibitors of mammalian G1 cyclin-dependent kinases. Genes Dev 1995;9(10):1149–63.
[30] Yew TL, Chiu FY, Tsai CC, Chen HL, Lee WP, Chen YJ, et al. Knockdown of p21Cip1/Waf1 enhances proliferation, the expression of stemness markers, and osteogenic potential in human mesenchymal stem cells. Aging Cell 2011;10(2):349–61.
[31] Premnath P, Jorgenson B, Hess R, Tailor P, Louie D, Taiani J, et al. p21−/− mice exhibit enhanced bone regeneration after injury. BMC Muscoskel Disord 2017;18(1):435.